A Supervisory Sliding Mode Control Approach for Cooperative Robotic Systems of Systems

Gian Paolo Incremona, *Member, IEEE,* Gianluca De Felici, Antonella Ferrara, *Senior Member, IEEE,* and Ezio Bassi

***Abstract*—This paper deals with the formulation of a supervisory sliding mode control approach oriented to deal with the interesting class of Systems of Systems (SoS) of robotic nature. This class of systems is characterized by the fact of being inherently distributed, cooperative and possibly heterogeneous. In this paper, we propose a modular and composable approach relying on basic modules featuring a multi-level functional architecture, including a supervisor and a couple of hybrid position/force control schemes associated with a couple of cooperative robotic manipulators. In principle, the overall robotic system we are referring to can be viewed as a collection of basic modules of that type. In the present paper, we focus on the design of the basic module. The hybrid position/force control schemes therein included are based on position and force controllers. The proposed position and force controllers are of Sliding Mode (SM) type, so as to assure suitable robustness to perform a satisfactory trajectory tracking even in presence of unavoidable modelling uncertainties and external disturbances. The verification and the validation of our proposal have been performed by simulating the supervisor and the hybrid control scheme applied to one of the two robotic manipulators, while experimentally testing the position control on the other arm. The experimental part of the tests has been carried out on a COMAU SMART3-S2 anthropomorphic industrial robotic manipulator.**

***Index Terms*—Systems of Systems (SoS), cooperative robotic system, Sliding Mode (SM) control, robotic manipulators.**

I. INTRODUCTION

RECENT advances in industry and research include the so-called *System of Systems* (SoS) concept, according to which the overall properties of a system of several, interconnected, also heterogeneous systems can be made even better than those of the sum of its parts [1], [2]. Also in robotics, this concept could be valid and kept into account during the design of control systems. In particular, it seems appropriate when one has to model and control cooperative robotic manipulators.

In a robotic cooperative control system, each component contributes to obtain a common goal, so as to perform tasks which could be too complex for being accomplished by a single robot, i.e. carrying heavy or large payloads, assembling multiple parts, handling flexible and critical objects. Moreover, the use of multiple robots increases the robustness of the system, and, in case the robots are resource-bounded, often turns out to be more convenient than the use of a single powerful robot [3].

In general, a distributed industrial robotic system can consist of a large number of robotic manipulators which could be expected to cooperate. Looking at the overall robotic system under a SoS perspective can allow one to conceive a modular and composable approach to design the whole control system. This is exactly the aim of the present paper in which we start from the identification of a *basic module*, define the control structure and the supervision logic associated with that module, design the controllers included in the control scheme, and provide the stability analysis of the resulting supervisory cooperative robot control approach. Then, the overall large scale and highly complex robotic system can be viewed as a collection of a (possibly large) number of basic modules, with guaranteed stability properties. The high level coordination among basic modules is outside the scope of the present work, but will be the object of future research.

As for the design of the controllers present in the basic module, it is worth recalling that various control approaches can be adopted to control a set of robotic manipulators. Such approaches can be classified in relation to the type of the task space and of the features of the object to manipulate. If the object is flexible and the task space is tridimensional, the *Virtual Linkage* approach [4] and the *Augmented Object* one [5], [6] can be adopted. On the contrary, if the object is rigid, and a planar task space is considered, the so-called *Symmetric formulation* and the *Virtual Stick* concept can be applied [7].

In this paper, the last two approaches are considered to deal with the two-robots cooperative system included in the basic module. For the sake of simplicity, the theoretical development hereafter reported, is referred to robotic manipulators which are planar and with three joints. However, the proposed control scheme and the design of the controllers could have a more general validity. According to a multi-level functional architecture, in the paper, a simple supervisor and a hybrid position/force control scheme for each robot are designed, on the base of the kinematical and dynamical models of the overall system, also including the object and the force sensors.

Inspired by [8], the low level controllers are designed according to the Sliding Mode (SM) approach [9], [10]. This choice has been suggested by the satisfactory performance illustrated in [11], even if in the different case of motion control of a single robot. Moreover, in the cooperative case, the effect of modelling uncertainties and external disturbances can be even more critical than in the conventional case, which makes the adoption of a robust control approach mandatory. The SM control approach provides well-known robustness features, and perfectly fits to solve the problem under concern. It presents, however, the notorious chattering effect [12], [13], [14], [15], which in past years has limited its use in robotics.

This is the final version of the accepted paper submitted to IEEE Systems Journal. G. P. Incremona, G. De Felici, A. Ferrara and E. Bassi are with the Dipartimento di Ingegneria Industriale e dell'Informazione, University of Pavia, Pavia 27100 Italy (e-mail: gp.incremona@gmail.com, {gianluca.defelici, antonella.ferrara, ezio.bassi}@unipv.it).

Nowadays, several chattering alleviation methods are available in literature (see, for instance, [16], [17], and the references therein cited). This is the reason why it is worth further investigating the design of SM based control schemes for robotic systems. Indeed, at the present stage of the research, SM robot controllers can be actually applicable in practice.

Note that, even if the cooperative control of robotic manipulators is a classical topic [3], to the best of our knowledge, this is the first paper in which SM control is applied to this context, and experimental results are reported. Further, the modular and composable SM based design here proposed, allowed by the SoS interpretation of the overall robotic system, is totally new.

The present paper is organized as follows. In Section II, a modular and composable approach, based on a multi-level functional architecture, is described. In Section III, the kinematical and dynamical models of a three joints planar robotic manipulator are introduced. In Section IV, the multi-robot system problem is formulated. In Section V, the *Symmetric formulation* and the *Virtual Stick* concept are applied to the considered cooperative system, and the safe grasp condition is defined. In Section VI, the basic module of the architecture is discussed. In Section VII, the proposed hybrid control scheme is described, while in Section VIII, the inverse dynamics approach is illustrated and the proposed Sliding Mode controllers are designed. The final part of the paper is devoted to present simulation and experimental results. These latter are obtained by running experimental tests on a COMAU SMART3-S2 anthropomorphic industrial robotic manipulator.

II. THE PROPOSED MODULAR AND COMPOSABLE DESIGN APPROACH

The robotic SoS we are dealing with consists of m robotic manipulators which, in principle, could be heterogeneous as for size, type (e.g. anthropomorphic, cartesian, spherical, cylindrical or SCARA manipulators), and complexity. They

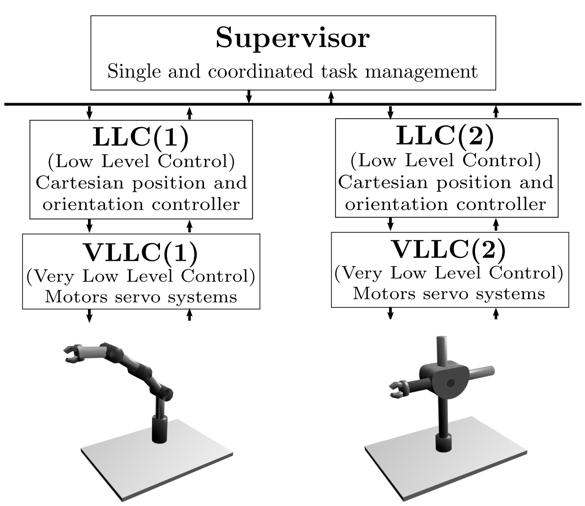

Figure 1. The basic module of the multi-level architecture for controlling the robotic SoS, in case of heterogeneous robots.

are expected to be controlled in a distributed way in order to perform, in a cooperative fashion, a high level common task.

The single robotic manipulator can be considered as the basic system, while a couple of cooperative controlled manipulators is the basic SoS. This latter can be depicted as in Figure 1, where the proposed distributed control multi-level architecture, inspired by [18], is also illustrated. It consists of three levels. From the bottom, one has the Very Low Level Control (VLLC) layer, in correspondence of which the robot system is feedback linearized, and the Low Level Control (LLC) layer, in correspondence of which the control algorithms are implemented, applied to the linearized system. The Supervisor layer has the function of coordinating the motion of each robot on the basis of the reference task. Then, relying on the basic module in Figure 1, a group of basic modules can be considered as a System of SoS (SoSoS), as shown in Figure 2. The SoSoS structure is not fixed, meaning that each block can be connected and disconnected, for instance, to be replaced in case of failure.

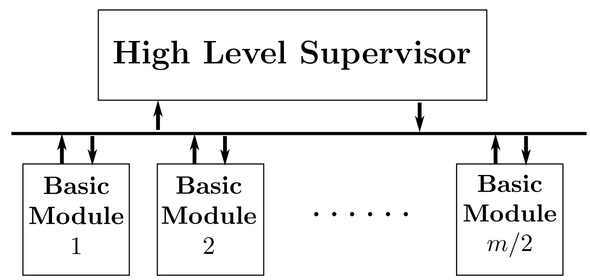

Figure 2. The overall SoSoS.

For the sake of simplicity, in this paper, we suppose that the two robotic manipulators of the basic module are homogeneous, as in Figure 3. Note, however, that the control scheme proposed

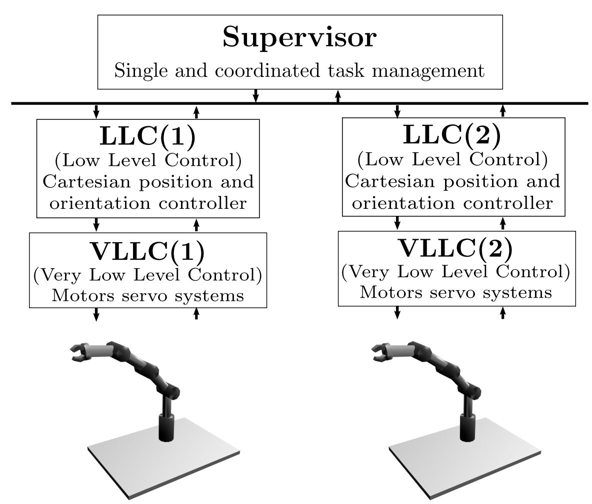

Figure 3. The basic module of the multi-level architecture for controlling the robotic SoS, in case of homogeneous robots. This is the case considered in the paper.

in this paper is valid also for the heterogeneous case, provided that the specific model of each manipulator is considered during the design phase.

In this paper, we focus on the design of the supervisory control of the basic module. Future research work will be devoted to devise a cooperation strategy to be implemented by a high level supervisor so as to attain more general and higher level objectives, e.g. a fair distribution of elementary tasks, of workload and, correspondently, of wear among the robotic basic modules.

III. SINGLE-ROBOT SYSTEM MODEL

In order to formulate the model of a n-joints rigid robotic manipulator, kinematical and dynamical aspects have to be considered. In this paper, only vertical planar motions of the robotic manipulator are enabled by locking three of the six joints of the robot (see Figure 4). In the next sections, $l_i,\ i = 1, 2, 3$, will denote the length of the i-th link, q_1 will denote the orientation of the first link with respect to $\boldsymbol{y}$-axis clockwise positive, and $q_j,\ j = 2, 3$, will denote the displacement of the j-th link with respect to the $(j-1)$-th one clockwise positive.

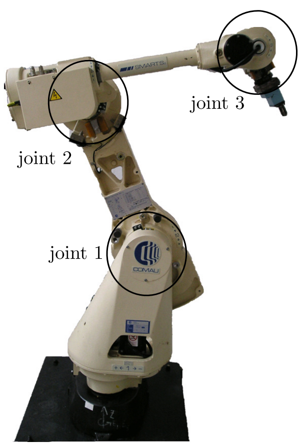

Figure 4. The COMAU SMART3-S2 anthropomorphic industrial robotic manipulator with the joints numeration.

In order to improve the readability of the paper, all the main notations are briefly described in Table I. For the sake of simplicity, the dependence of all the variables on joint variables $\boldsymbol{q}$, and on time t will be omitted, when it is obvious.

A. Kinematics

It is well known that the kinematics of a three joints manipulator describes the relationship between the joint variables $\boldsymbol{q} = [q_1\ q_2\ q_3]^T$ and the end-effector position and orientation $\boldsymbol{x} = [p_x\ p_y\ \phi]^T$ in the planar workspace. With reference to Figure 4, the direct kinematics equations in our case are given by

$$\begin{cases} p_x = l_1 \sin(q_1) + l_2 \sin(q_1 + q_2) + l_3 \sin(\phi) \\ p_y = l_1 \cos(q_1) + l_2 \cos(q_1 + q_2) + l_3 \cos(\phi) \\ \phi = q_1 + q_2 + q_3 \end{cases} \quad (1)$$

Table I
NOTATIONS.

$\boldsymbol{q}(t)$	joint variables, (3×1)
$\boldsymbol{x}(\boldsymbol{q})$	position/orientation of the j-th end-effector, (3×1)
$\boldsymbol{\tau}(t)$	motors torques w.r.t. the joint space, (3×1)
$\boldsymbol{J}(\boldsymbol{q})$	geometric/analytic Jacobian, (3×3)
$\boldsymbol{\gamma}(t)$	motors torques w.r.t. the operative space, (3×1)
$\boldsymbol{p}_j(\boldsymbol{q})$	position of the j-th end-effector, (2×1)
$\phi_j(t)$	orientation of the j-th end-effector
$\boldsymbol{r}_j(t)$	j-th virtual stick w.r.t. the base frame, (2×1)
$\boldsymbol{p}_C(t)$	position of the object center of mass, (2×1)
$\boldsymbol{p}_{S,j}(t)$	position of the j-th stick, (2×1)
$\boldsymbol{h}_j(t)$	generalized forces on the j-th end-effector, (6×1)
$\boldsymbol{f}_j(t)$	forces applied on the j-th end-effector, (3×1)
$\boldsymbol{\mu}_j(t)$	torques applied on the j-th end-effector, (3×1)
$\boldsymbol{h}_E(t)$	external forces causing the motion of the object, (6×1)
$\boldsymbol{p}_E(\boldsymbol{q})$	absolute position of the end-effectors, (2×1)
$\phi_E(t)$	absolute orientation of the end-effectors
$\boldsymbol{p}_I(\boldsymbol{q})$	relative position of the end-effectors, (2×1)
$\phi_I(t)$	relative orientation of the end-effectors
$\boldsymbol{f}_E(t)$	external forces applied on the object, (3×1)
$\boldsymbol{\mu}_E(t)$	external torques applied on the object, (3×1)
$\boldsymbol{f}_{sf}(t)$	static friction force, (3×1)
$\boldsymbol{x}_{d,j}(t)$	desired position/orientation of the j-th end-effector, (3×1)
$\boldsymbol{x}_e(t)$	equilibrium pose of the object contact surface, (3×1)
$\tilde{\boldsymbol{y}}(t)$	auxiliary control variable w.r.t. the operative space, (3×1)
$\boldsymbol{y}(t)$	auxiliary control variable w.r.t. the joint space, (3×1)

B. Dynamics

The dynamics of the robot can be written in the joint space, by using the Lagrangian approach, as

$$\boldsymbol{B}(\boldsymbol{q})\ddot{\boldsymbol{q}} + \boldsymbol{n}(\boldsymbol{q}, \dot{\boldsymbol{q}}) = \boldsymbol{\tau} - \boldsymbol{J}^T(\boldsymbol{q})\boldsymbol{h} \quad (2)$$

$$\boldsymbol{n}(\boldsymbol{q}, \dot{\boldsymbol{q}}) = \boldsymbol{C}(\boldsymbol{q}, \dot{\boldsymbol{q}})\dot{\boldsymbol{q}} + \boldsymbol{F}_v\dot{\boldsymbol{q}} + \boldsymbol{F}_s \boldsymbol{sgn}(\dot{\boldsymbol{q}}) + \boldsymbol{g}(\boldsymbol{q}) \quad (3)$$

where $\boldsymbol{B}(\boldsymbol{q}) \in \mathbb{R}^{3\times3}$ is the inertia matrix, $\boldsymbol{C}(\boldsymbol{q}, \dot{\boldsymbol{q}}) \in \mathbb{R}^{3\times3}$ represents centripetal and Coriolis torques, $\boldsymbol{F}_v \in \mathbb{R}^{3\times3}$ is the viscous friction matrix, $\boldsymbol{F}_s \in \mathbb{R}^{3\times3}$ is the static friction matrix, $\boldsymbol{g}(\boldsymbol{q}) \in \mathbb{R}^3$ is the vector of gravitational torques and $\boldsymbol{\tau} - \boldsymbol{J}^T(\boldsymbol{q})\boldsymbol{h} \in \mathbb{R}^3$ represents the motors torques and the interaction of the end-effector with the environment.

IV. MULTI-ROBOT SYSTEM MODEL

To control multiple robots, the overall system has to be referred to a common base frame. Moreover, kinematics and dynamics have to be considered in terms of joint variables and operative space variables. In this paper, to limit the complexity of the cooperative system, only a two-robots system is discussed (see Figure 5). Note that each robot manipulator is a robot of the type described in Section III.

The main relationship between the dynamical model in the joint space and that in the operative space, for a non-redundant manipulator, can be written as

$$\boldsymbol{\tau} = \boldsymbol{J}^T\boldsymbol{\gamma} \quad (4)$$

where $\boldsymbol{J} \in \mathbb{R}^{3\times3}$ is the analytic or geometric Jacobian and $\boldsymbol{\gamma} \in \mathbb{R}^3$ is the vector of the torques in the operative space [19].

V. PROBLEM FORMULATION

A. Preliminary Issues

Consider Figure 5. Let $O - \{\boldsymbol{x}, \boldsymbol{y}, \boldsymbol{z}\}$ denote the base frame so that the center O is placed at the same distance from the two manipulators. Let ${}^jO_0 - \{\boldsymbol{x}_0, \boldsymbol{y}_0, \boldsymbol{z}_0\}$, $j = 1, 2$, denote the 0-frame of the j-th robotic manipulator, so that the center ${}^jO_0$ is placed in the centre of the first joint of each robot. Let ${}^jO_e - \{\boldsymbol{n}, \boldsymbol{s}, \boldsymbol{a}\}$ denote the end-effector frame of the j-th robotic manipulator, so that the center ${}^jO_e$ is placed on the its end-effector, and the axes $\{\boldsymbol{n}, \boldsymbol{s}, \boldsymbol{a}\}$ are indicated in Figure 5. Let $O_\mathrm{C} - \{\boldsymbol{x}_\mathrm{C}, \boldsymbol{y}_\mathrm{C}, \boldsymbol{z}_\mathrm{C}\}$ denote the object frame with the center O_C in the center of mass of the object.

The direct kinematics of each robotic manipulator can be written as

$$\begin{cases} \boldsymbol{p}_j = \boldsymbol{p}_j({}^j\boldsymbol{q}) \\ \phi_j = {}^jq_1 + {}^jq_2 + {}^jq_3 \end{cases} \tag{5}$$

where $\boldsymbol{p}_j = [p_{j,x}\ p_{j,y}]^T$ is the position of the j-th end-effector and ϕ_j is its orientation.

To define the position of each end-effector with respect to a rigid object, one can use the *virtual stick* $\boldsymbol{r}_j$ with respect to the base frame (see Figure 5). Each rigid stick is placed on the j-th end-effector, while the position of the object, given by $\boldsymbol{p}_\mathrm{C}$, and the position of the tip of the j-th stick, given by $\boldsymbol{p}_{S,j}$, are defined as

$$\boldsymbol{p}_\mathrm{C} = \boldsymbol{p}_j + \boldsymbol{r}_j = \boldsymbol{p}_{S,j}. \tag{6}$$

Considering the rotation matrix $\boldsymbol{R}_\mathrm{C} \in \mathbb{R}^{3\times3}$ between the object frame and the base one, the direct kinematics of the whole system can be written as

$$\begin{cases} \boldsymbol{p}_\mathrm{C} = \boldsymbol{p}_{S,j} \\ \boldsymbol{R}_\mathrm{C} = \boldsymbol{R}_{S,j} \end{cases} \tag{7}$$

where $\boldsymbol{R}_{S,j}$ is a function of a set of Euler angles, given by $\phi_{S,j}$ [3].

The *Symmetric formulation* describes the main relationships between the generalized forces and velocities on the manipulated object and the generalized forces and velocities from the point of view of the end-effectors and of the virtual sticks [7]. Let $\boldsymbol{h}_j = [\boldsymbol{f}_j^T\ \boldsymbol{\mu}_j^T]^T \in \mathbb{R}^6$ denote the vector of the generalized forces acting on the j-th end-effector. The generalized forces acting on the tip of the j-th virtual stick can be written as

$$\boldsymbol{h}_{S,j} = \begin{bmatrix} \boldsymbol{I}_3 & \boldsymbol{0}_3 \\ -\boldsymbol{S}(\boldsymbol{r}_j) & \boldsymbol{I}_3 \end{bmatrix} \boldsymbol{h}_j = \boldsymbol{W}_j \boldsymbol{h}_j \tag{8}$$

where $\boldsymbol{W}_j \in \mathbb{R}^{6\times6}$ is always full rank, $\boldsymbol{I}_3 \in \mathbb{R}^{3\times3}$ is the identity matrix, $\boldsymbol{0}_3 \in \mathbb{R}^{3\times3}$ is the null matrix, and $\boldsymbol{S}(\boldsymbol{r}_j) \in \mathbb{R}^{3\times3}$ is the skew-symmetric matrix operator for the cross product $\boldsymbol{r}_j \times \boldsymbol{f}_j$. According to the principle of virtual work, it is possible to write the equivalent relationship for the velocity [3]. In our case such relationship is useless, and so it is omitted.

The external forces causing the motion of the object can be written as

$$\boldsymbol{h}_E = \boldsymbol{h}_1 + \boldsymbol{h}_2 = \boldsymbol{W}\boldsymbol{h} \tag{9}$$

where $\boldsymbol{W} = [\boldsymbol{W}_1\ \boldsymbol{W}_2] \in \mathbb{R}^{6\times12}$ is the grasp matrix, and $\boldsymbol{h} = [\boldsymbol{h}_1^T\ \boldsymbol{h}_2^T]^T \in \mathbb{R}^{12}$ is the force vector applied by the two robots. The inverse problem can be solved as

$$\boldsymbol{h} = \boldsymbol{W}^\dagger \boldsymbol{h}_E + \boldsymbol{V}\boldsymbol{h}_I = \boldsymbol{U}\boldsymbol{h}_O \tag{10}$$

where $\boldsymbol{W}^\dagger \in \mathbb{R}^{12\times6}$ is the Moore-Penrose pseudo-inverse of $\boldsymbol{W}$, $\boldsymbol{V} \in \mathbb{R}^{12\times6}$ represents the null space of $\boldsymbol{W}$, such that $\boldsymbol{h}_I \in \mathbb{R}^6$ is the vector of the generalized internal forces which do not generate motions of the object.

The absolute position and orientation of the object in terms of the end-effectors positions can be written as

$$\begin{cases} \boldsymbol{p}_E = \frac{1}{2}\left(\boldsymbol{p}_{S,1} + \boldsymbol{p}_{S,2}\right) \\ \phi_E = \frac{1}{2}\left(\phi_{S,1} + \phi_{S,2}\right) \end{cases} \tag{11}$$

while the relative ones are given by

$$\begin{cases} \boldsymbol{p}_I = \boldsymbol{p}_{S,2} - \boldsymbol{p}_{S,1} \\ \phi_I = \phi_{S,2} - \phi_{S,1} \end{cases} \tag{12}$$

The dynamics of the whole system includes the two robots dynamics, according to Equation (2), and also the dynamical model of the object, given by

$$\begin{cases} m\ddot{\boldsymbol{p}}_E = -\boldsymbol{g}_E + \boldsymbol{f}_E + \boldsymbol{f}_{sf} \\ \boldsymbol{R}_E \mathbf{I}_\mathrm{C} \boldsymbol{R}_E^T \ddot{\phi}_E = -\dot{\phi}_E \times (\boldsymbol{R}_E \mathbf{I}_\mathrm{C} \boldsymbol{R}_E^T \dot{\phi}_E) + \boldsymbol{\mu}_E \end{cases} \tag{13}$$

where $\boldsymbol{g}_E \in \mathbb{R}^3$ is the vector of the gravitational forces, $\boldsymbol{f}_E \in \mathbb{R}^3$ is the external force vector, $\boldsymbol{f}_{sf} \in \mathbb{R}^3$ is the static friction force vector, $\boldsymbol{R}_E = \boldsymbol{R}_\mathrm{C}$ is the rotation matrix between the object frame and the base one, $\mathbf{I}_\mathrm{C}$ is the tensor of inertia with respect to the object center of mass, and $\boldsymbol{\mu}_E$ is the vector of the applied external torques.

B. Safe Grasp Concept and Safe Grasp Condition

At this point, the introduction of a new notion seems advisable. This is the notion of *safe grasp*, that is the minimum value of the applied forces, $\boldsymbol{h}_{sg}$ such that the object is tightly attached to each end-effector.

In the next section this notion will be specified relying on the particular task which is considered, as an example, during the design of the proposed control system.

C. Problem Statement

We are now in a position to be able to formulate the control problem to solve.

Given the two-robots system described in Section IV, starting from an initial condition of safe grasp, the aim of the control system to be designed is to make the cooperative robot system perform simple tasks, while fulfilling the safe grasp condition uniformly in time, i.e.

$$\boldsymbol{h}_j \geq \boldsymbol{h}_{sg},\ j = 1, 2 \qquad \forall t \geq t_0 \tag{14}$$

where t_0 is the initial time instant.

In the following section, a functional architecture including a supervisor is introduced. The role of the supervisor is that of providing the reference trajectories for each robot, starting from the definition of the high-level task to be performed.

VI. THE BASIC MODULE OF THE ARCHITECTURE

In this section the basic module of the functional architecture to control the robotic system of systems under concern is presented. The structure is that already introduced in Figure 3.

Our proposal of supervisor is simple but sufficient to give rise to an effective overall cooperative control scheme. Given (11)-(12) which are the absolute and relative position and orientation of the object, the supervisor produces a reference position and orientation for the j-th robot. More specifically for our robot

$$\boldsymbol{x}_{d,j} = \begin{bmatrix} \boldsymbol{p}_{E_d} - \boldsymbol{r}_j \pm \frac{\boldsymbol{p}_{I_d}}{2} \\ \phi_{E_d} \pm \frac{\phi_{I_d}}{2} \end{bmatrix} \tag{15}$$

taking into consideration that $\boldsymbol{p}_{I_d} = \mathbf{0}$ as well as $\phi_{I_d} = \pi$. As for the generation of the force reference, note that, for the sake of simplicity, to run the experimental and simulation tests reported in Section IX, an elementary task has been considered, consisting in moving the object along an horizontal line parallel to the $\boldsymbol{x}$-axis of the base frame. As for this task, relying on system (13), considering the torques acting on the object negligible, as well as $\ddot{\boldsymbol{p}}_E = \mathbf{0}$ and $\phi_E = 0$, so as to actually move the object horizontally, the corresponding *safe grasp condition* can be expressed as follows

$$\boldsymbol{h}_{sg} = \begin{bmatrix} \frac{Mg}{2\mu_s} \\ 0 \end{bmatrix} \tag{16}$$

where M is the mass of the object, μ_s is the static friction on the contact surface, and $g = 9.81\,\mathrm{m\,s^{-2}}$. Even if a simple task is hereafter considered, all the theoretical developments and all the control solutions discussed in this paper also hold for more complex tasks.

VII. THE PROPOSED SLIDING MODE HYBRID POSITION/FORCE SCHEME

In Figure 6 the proposed control scheme for each robot is illustrated. Note that $\boldsymbol{\Sigma}_p$ and $\boldsymbol{\Sigma}_h = \boldsymbol{I}_3 - \boldsymbol{\Sigma}_p$ are conventional selection matrices, i.e. they allow to distinguish between the directions along which the position control and the force control are performed [20]. In the considered case, they are defined as

$$\boldsymbol{\Sigma}_p = \begin{bmatrix} 1 & 0 & 0 \\ 0 & 0 & 0 \\ 0 & 0 & 1 \end{bmatrix}, \quad \boldsymbol{\Sigma}_h = \begin{bmatrix} 0 & 0 & 0 \\ 0 & 1 & 0 \\ 0 & 0 & 0 \end{bmatrix} \tag{17}$$

This scheme includes two feedback loops. The first one is designed for the position tracking control, the desired position being generated by the supervisor and compared with the position determined by transforming the measured angular positions through system (1), i.e. $\boldsymbol{k}(\boldsymbol{q})$. Controller C_1 computes the position control variable $\tilde{\boldsymbol{y}}_p$. The second feedback loop is specifically designed for the force control. The force $\boldsymbol{h}_O$, which includes the generalized forces applied by the two manipulators, is detected by the force sensor. Then, this is transformed, relying on the *Symmetric formulation*, according to Equation (10). The internal forces of the object $\boldsymbol{h}_I$ are considered negligible, so that one has

$$\boldsymbol{h} = \boldsymbol{W}^{\dagger}\boldsymbol{h}_O \tag{18}$$

where $\boldsymbol{W}^{\dagger} = [\frac{1}{2}\boldsymbol{I}_2 \;\; \frac{1}{2}\boldsymbol{I}_2]^T \in \mathbb{R}^{4\times 2}$ is the pseudo inverse of the grasp matrix $\boldsymbol{W} = [\boldsymbol{I}_2 \;\; \boldsymbol{I}_2] \in \mathbb{R}^{2\times 4}$. Note that in Figure 6, the expression $\boldsymbol{h}_j \leftarrow \boldsymbol{h}_O$ indicates that only the generalized forces of the j-th robot are used, while $\hat{\boldsymbol{h}}_{c,j} \leftarrow \boldsymbol{h}_j$ indicates that only the contact force is selected according to [8]. Only the first two components of the force are used. Moreover, we assume that the interaction between each robot and the object is described by the virtual spring model

$$\boldsymbol{h} = \boldsymbol{K}_S(\boldsymbol{x} - \boldsymbol{x}_e) \tag{19}$$

where $\boldsymbol{x}_e = [\boldsymbol{p}_e^T \;\; \phi_e]^T$ is the equilibrium position and orientation of the contact surface between the object and the end-effector.

The inverse of the diagonal positive definite matrix $\boldsymbol{K}_S$ is used to transform the force tracking error $\boldsymbol{e}_h^{(\Sigma)} = \boldsymbol{\Sigma}_h\boldsymbol{e}_h$, where $\boldsymbol{e}_h = [(\boldsymbol{h}_{sg} - \boldsymbol{h})^T \;\; 0]^T \in \mathbb{R}^3$, into $\boldsymbol{e}_p^{h,(\Sigma)}$, which is dimensionally a position error. Controller C_2 computes the force control variable $\tilde{\boldsymbol{y}}_h$. Then, the auxiliary input signal $\tilde{\boldsymbol{y}}$ is obtained as

$$\tilde{\boldsymbol{y}} = \tilde{\boldsymbol{y}}_p + \tilde{\boldsymbol{y}}_h \tag{20}$$

Note that, in the scheme in Figure 6, by using the second order differential kinematics equation, one has

$$\boldsymbol{y} = \boldsymbol{J}^{-1}(\tilde{\boldsymbol{y}} - \dot{\boldsymbol{J}}\dot{\boldsymbol{q}}) \tag{21}$$

The proposed control scheme allows one to implement, as position and force controllers, two position controllers.

VIII. DESIGN OF LOW LEVEL (LLC) AND VERY LOW LEVEL CONTROL (VLLC)

In this section the LLC and VLLC parts of the proposed control scheme for each robotic manipulator are presented.

A. VLLC: Inverse Dynamics Controller

To design the VLLC part of the proposed scheme, the classical inverse dynamics control approach [20] has been followed. The inverse dynamics of a rigid robot manipulator can be written in the joint space as a non linear relationship between the plant inputs and the plant outputs, relying on (2)-(3), so that the control law results in being

$$\boldsymbol{\tau} = \boldsymbol{B}(\boldsymbol{q})\boldsymbol{y} + \hat{\boldsymbol{n}}(\boldsymbol{q}, \dot{\boldsymbol{q}}) + \boldsymbol{J}^T(\boldsymbol{q})\boldsymbol{h} \tag{22}$$

where $\boldsymbol{y}$ is an auxiliary control variable obtained as in (21). Note that $\boldsymbol{B}(\boldsymbol{q})$ and $\hat{\boldsymbol{n}}$ need to be identified on the basis of experimental tests. In our work, we assume that the identified $\boldsymbol{B}(\boldsymbol{q})$ coincides with the actual one (it is a quite accurate replica), which, on the basis of our experience, is often true in practice, while $\hat{\boldsymbol{n}}$ is an estimate of $\boldsymbol{n}$, which does not necessarily coincide with $\boldsymbol{n}$. In the following we make reference to the experimentally identified $\boldsymbol{B}(\boldsymbol{q})$ and $\hat{\boldsymbol{n}}$ in [21]. By applying the feedback linearization to the system (2)-(3), one obtains

$$\ddot{\boldsymbol{q}} = \boldsymbol{y} + \boldsymbol{B}^{-1}(\boldsymbol{q})\tilde{\boldsymbol{n}}(\boldsymbol{q}, \dot{\boldsymbol{q}}) = \boldsymbol{y} - \boldsymbol{\eta}(\boldsymbol{q}, \dot{\boldsymbol{q}}) \tag{23}$$

where $\boldsymbol{\eta}(\boldsymbol{q}, \dot{\boldsymbol{q}})$ takes into account the modelling uncertainties and dynamical effects, and

$$\tilde{\boldsymbol{n}}(\boldsymbol{q}, \dot{\boldsymbol{q}}) = \hat{\boldsymbol{n}}(\boldsymbol{q}, \dot{\boldsymbol{q}}) - \boldsymbol{n}(\boldsymbol{q}, \dot{\boldsymbol{q}}) \tag{24}$$

B. LLC: Sliding Mode based Position/Force Controllers

The design of the LLC part of the proposed control scheme for each robot is based on the Sliding Mode control approach.

According to this latter, two sliding functions are selected as

$$\boldsymbol{s}_p(t) = m_p \boldsymbol{e}_p^{(\Sigma)}(t) + \dot{\boldsymbol{e}}_p^{(\Sigma)}(t) \tag{25}$$

$$\boldsymbol{s}_h(t) = m_h \boldsymbol{e}_p^{h,(\Sigma)}(t) + \dot{\boldsymbol{e}}_p^{h,(\Sigma)}(t) \tag{26}$$

where $m_p, m_h \in \mathbb{R}$ are scalars, and $\boldsymbol{e}_p^{(\Sigma)}$, $\boldsymbol{e}_p^{h,(\Sigma)}$ are the position and transformed force error, respectively, indicated in Figure 6. Then, the two terms which form the auxiliary input signal are designed as

$$\tilde{\boldsymbol{y}}_p(t) = \boldsymbol{K}_p \mathbf{sgn}(\boldsymbol{s}_p(t)) \tag{27}$$

$$\tilde{\boldsymbol{y}}_h(t) = \boldsymbol{K}_h \mathbf{sgn}(\boldsymbol{s}_h(t)) \tag{28}$$

where $\boldsymbol{K}_p,\ \boldsymbol{K}_h \in \mathbb{R}^{3\times 3}$ are diagonal matrices and $\mathbf{sgn}(\cdot) \in \mathbb{R}^3$.

With reference to the proposed control law, the following results can be proved.

Theorem 1: Given system (2)-(3), with the kinematics equations in (1), controlled via the inverse dynamics based VLLC in (22), and the LLC laws in (27)-(28), assume that the reference signals $\boldsymbol{x}_d$ and $\boldsymbol{h}_{sg}$ are C^2, known and bounded with known and bounded derivatives, then the position error $\boldsymbol{e}_p(t)$ and the force error $\boldsymbol{e}_h(t)$ are asymptotically steered to zero in spite of the presence of the uncertainty $\boldsymbol{\eta}(\boldsymbol{q}, \dot{\boldsymbol{q}})$.

Proof: Consider the sliding functions $\boldsymbol{s}_p(t)$ and $\boldsymbol{s}_h(t)$ in (25)-(26). Their first time derivatives, omitting the dependence on time when obvious, can be written as

$$\dot{\boldsymbol{s}}_p(t) = \boldsymbol{\Sigma}_p(\ddot{\boldsymbol{x}}_d + m_p \dot{\boldsymbol{e}}_p + \boldsymbol{J}\boldsymbol{\eta} - \tilde{\boldsymbol{y}}_p) \tag{29}$$

$$\dot{\boldsymbol{s}}_h(t) = \boldsymbol{\Sigma}_h(\ddot{\boldsymbol{x}}_e + m_h \boldsymbol{K}_S^{-1} \dot{\boldsymbol{e}}_h + \boldsymbol{J}\boldsymbol{\eta} - \tilde{\boldsymbol{y}}_h) \tag{30}$$

where $\boldsymbol{x}_e$ as in (19). Relying on (27) and (28), as well as on (29) and (30), one has that

$$\dot{s}_{p_i}(t) \leq -\eta_p \,\mathrm{sgn}(s_{p_i}(t)) \tag{31}$$

$$\dot{s}_{h_i}(t) \leq -\eta_h \,\mathrm{sgn}(s_{h_i}(t)) \tag{32}$$

where $\dot{s}_{p_i}(t),\ \dot{s}_{h_i}(t)\ s_{p_i}(t)\ s_{h_i}(t)$ are the i-th components of the corresponding signals, and η_p and η_h are positive constants related to $\boldsymbol{K}_p$ and $\boldsymbol{K}_h$, in (27)-(28), according to the following relationship

$$K_{p_{ii}} \geq \sum_{j=1}^{3} J_{ij}\eta_j + \eta_p + \ddot{x}_{d_i} + m_p \dot{e}_{p_i} \tag{33}$$

$$K_{h_{ii}} \geq \sum_{j=1}^{3} J_{ij}\eta_j + \eta_h + \ddot{x}_{e_i} + m_h K_{S_{ii}}^{-1} \dot{e}_{h_i} \tag{34}$$

where the terms $\ddot{x}_{d_i}$ is bounded by assumption, and the terms $\dot{e}_{p_i},\ \ddot{x}_{e_i}$ and $\dot{e}_{h_i}$ are bounded because of physical considerations (i.e. the robot actuators only provide bounded speeds and accelerations). This means that the so-called reaching condition [10] turns out to be fulfilled for both the sliding functions. This implies that $\boldsymbol{s}_p(t)$ and $\boldsymbol{s}_h(t)$ are steered to zero in a finite time t_r. From (25) and (26), it follows that, for $t \geq t_r$, the reaching errors $\boldsymbol{e}_p(t)$ and $\boldsymbol{e}_h(t)$ are asymptotically vanishing, which concludes the proof. ■

On the basis of Theorem 1, one can observe that, starting from a safe grasp condition, such a condition is ensured and maintained by the control scheme associated with each robot $\forall\, t \geq t_0$, t_0 being the initial time instant.

Theorem 2: Given the cooperative robot system illustrated in Figure 5, controlled via the functional architecture in Figure 3, with the LLC and VLLC for each robot as in Figure 6, assume that an absolute reference position $\boldsymbol{p}_{E_d}$ and orientation ϕ_{E_d} for the object to be manipulated, both of class C^2, are known at any time instant with their time derivatives, then, by starting at the initial time instant from a safe grasp condition, the safe grasp condition is maintained $\forall\, t \geq t_0$, and the object position and orientation are tracked asymptotically.

Proof: The initial condition of safe grasp implies that the sliding function $\boldsymbol{s}_h(t_0) = \mathbf{0}$. So, as for the force control problem one has that the sliding condition is ensured in $t = t_0$. By using Theorem 1, one can also prove that a sliding mode is enforced on the manifold $\boldsymbol{s}_h(t)$ for any $t \geq t_0$, since the sliding condition is guaranteed $\forall\, t \geq t_0$. As for the object position control problem, again relying on Theorem 1, one has that the reference signals $\boldsymbol{x}_{d,j}$ for $j = 1, 2$ are tracked asymptotically. Then, since (15) holds, one can conclude that also $\boldsymbol{p}_{E_d}$ and ϕ_{E_d} are tracked asymptotically, which proves the theorem. ■

IX. SIMULATION AND EXPERIMENTAL RESULTS

In this section the simulation and experimental results are discussed.

A. The Considered Simulation/Experimental Set-Up

Since in our lab only one industrial robot is actually present, the verification and validation of the idea underlying the proposal of this paper have been performed by simulating the supervisor and the hybrid control scheme applied to one of the two robotic manipulators, and by experimentally testing on a COMAU SMART3-S2 industrial anthropomorphic rigid robotic manipulator the position control loop. In practice, the experiments are carried on by considering at the same time the motion of the physical robot (the SMART3-S2) and that of the virtual robot (which is simulated relying on its identified model), as indicated in Figure 7. The SMART3-S2 robot consists of six links and six rotational joints driven by brushless electric motors, but only three joints are used to attain our purposes. To acquire the joints positions, resolvers are fastened on the three motors and the controller has got a minimum sampling time of $0.001\,\mathrm{s}$.

B. Verification and validation

The simulated initial configuration is shown in Figure 8. As previously mentioned, only planar motions are generated and we suppose that the safe grasp condition is verified at initial time instant. The distance of each robotic manipulator from the origin of the base frame is $d/2$. We perform the experimental tests on the robotic manipulator on the left (see Figure 14) while we simulate the robot on the right.

In order to assess the performance of the proposed supervisory hybrid sliding mode control scheme, the comparison with the performance obtained by replacing the SM based low level controllers with conventional PD controllers is also discussed in the following.

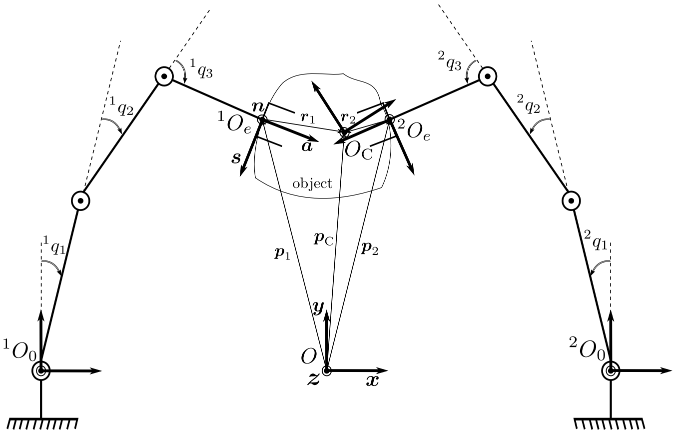

Figure 5. The considered two-robots system manipulating an object.

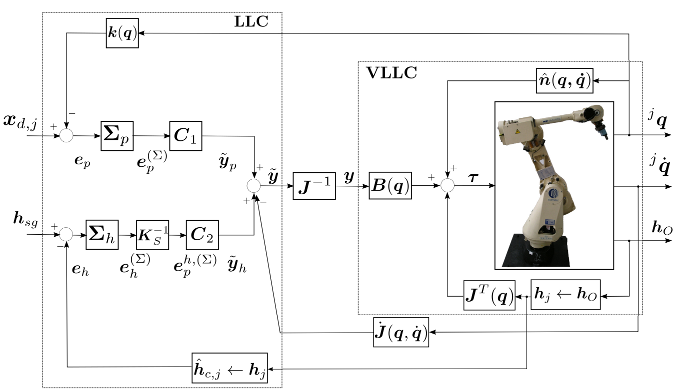

Figure 6. The hybrid position/force control scheme with the feedback linearization applied to the robot system.

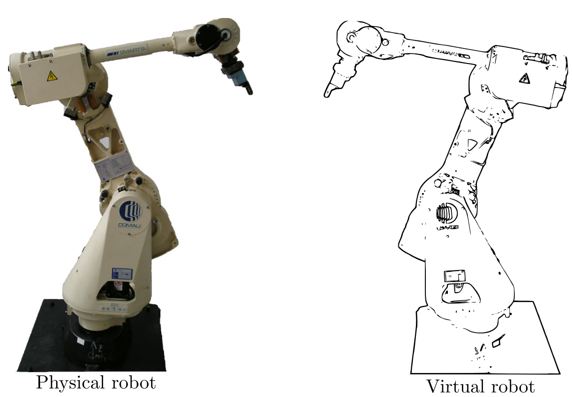

Figure 7. The physical robot and the virtual robot COMAU SMART3-S2.

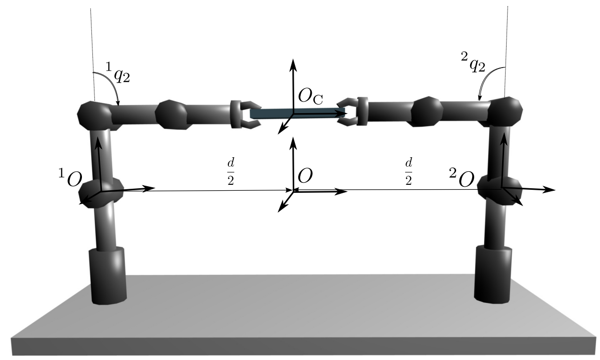

Figure 8. The simulated initial configuration of the two-robots system with the object tightly grasped by the end-effectors.

The PD controllers are designed so that

$$\tilde{\boldsymbol{y}}_p(t) = \boldsymbol{K}_{P,p}\boldsymbol{e}_p^{(\Sigma)}(t) + \boldsymbol{K}_{D,p}\dot{\boldsymbol{e}}_p^{(\Sigma)}(t) \tag{35}$$

$$\tilde{\boldsymbol{y}}_h(t) = \boldsymbol{K}_{P,h}\boldsymbol{e}_p^{h,(\Sigma)}(t) + \boldsymbol{K}_{D,h}\dot{\boldsymbol{e}}_p^{h,(\Sigma)}(t) \tag{36}$$

where $\boldsymbol{K}_{P,p},\ \boldsymbol{K}_{D,p},\ \boldsymbol{K}_{P,h},\ \boldsymbol{K}_{D,h} \in \mathbb{R}^{3\times 3}$ are diagonal matrices which stabilize the closed loop system [20]. The parameters used for the simulations and experimental tests are reported in Table II and III.

Table II
PD POSITION/FORCE CONTROL PARAMETERS FOR SIMULATIONS AND EXPERIMENTS.

$\boldsymbol{K}_{P,p}$	$\boldsymbol{K}_{D,p}$	$\boldsymbol{K}_{P,h}$	$\boldsymbol{K}_{D,h}$
400	35	10	4
450	35	40	4
350	35	-	-

Table III
SM POSITION/FORCE CONTROL PARAMETERS FOR SIMULATIONS AND EXPERIMENTS.

m	$\boldsymbol{K}_p$	$\boldsymbol{K}_h$
5	10	1
5	10	1
5	10	-

Moreover, to verify the robustness properties of the SM controllers, uncertainties $\boldsymbol{\xi} = [\xi_1\ \xi_2\ \xi_3]^T$ of the following types

$$\begin{cases} \xi_1 = 2\sin(10t) + \sin(20t) + 0.6\sin(30t) \\ \xi_2 = 8\sin(10t) + 4\sin(20t) + 2.5\sin(30t) \\ \xi_3 = 10\sin(10t) + 5\sin(20t) + 3\sin(30t) \end{cases} \tag{37}$$

have been added to the angular accelerations of the joints of the simulated robot (that on the right). Figure 9 and 10 show the trajectories of the end-effectors, respectively for the real robot and for the virtual one while the object is moved. Figure 11 and 12 show the corresponding behavior of the joint variables. Table IV and Figure 13 show the position/orientation (left bar chart) and force (right bar chart) Root Mean Square (RMS) errors, respectively in the case of PD and SM controllers without uncertainties, and in their presence. As it can be noted, satisfactory results are obtained. In particular, the proposed control approach allows one to obtain small tracking errors.

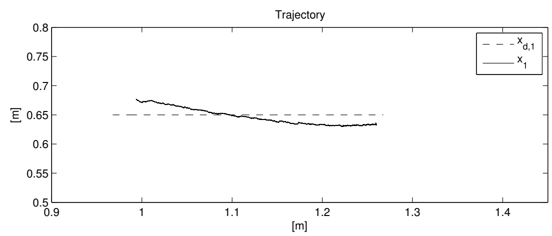

Figure 9. Motion of the end-effector of the robot on the left in the planar workspace when SM control is used in the experiments.

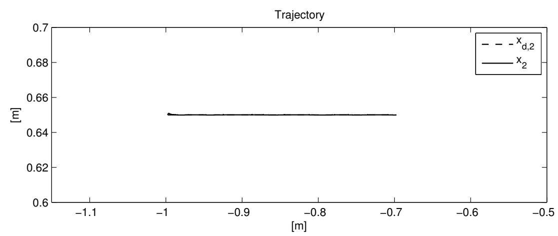

Figure 10. Motion of the end-effector of the robot on the right in the planar workspace when a SM control is used in the simulations.

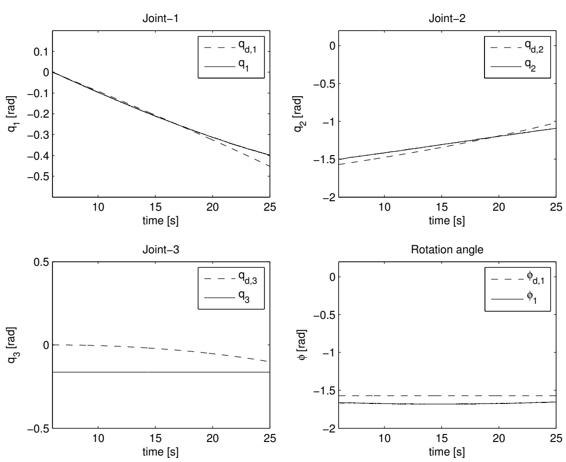

Figure 11. Joint variables and end-effector orientation of the robot on the left when a SM control is used in the experiments.

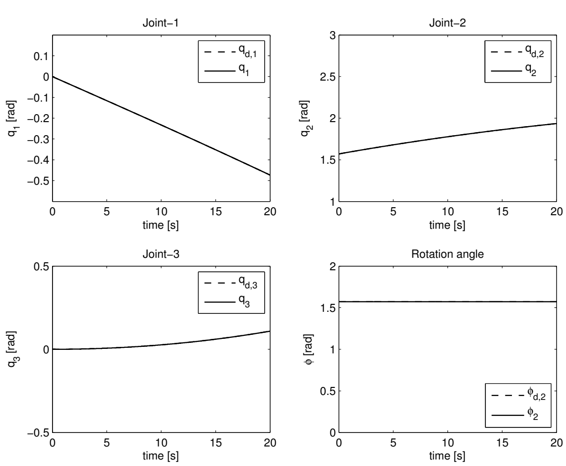

Figure 12. Joint variables and end-effector orientation of the robot on the right when a SM control is used in the simulations.

Table IV
RMS VALUES OF $\boldsymbol{e}_p$ AND $\boldsymbol{e}_h$ (SIMULATION RESULTS).

C_1/C_2	$e_{p_{RMS}}$	$e_{h_{RMS}}$
PD *(1)*	5.9056×10^{-4}	0.0049
PD^u *(2)*	0.0025	0.0202
SM *(3)*	2.7119×10^{-5}	5.6793×10^{-4}
SM^u *(4)*	7.6518×10^{-5}	5.0986×10^{-4}

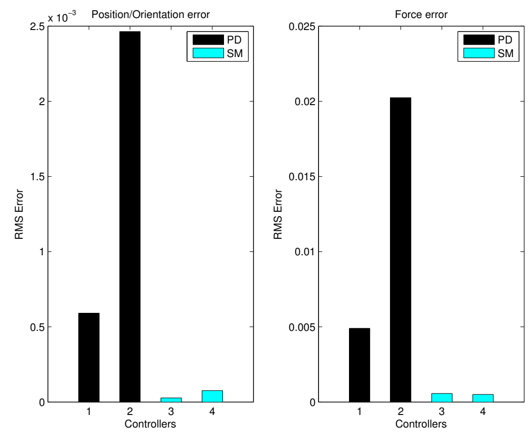

Figure 13. Comparison of the RMS values of the position/orientation and force errors of the end-effector of the robot on the right using PD and SM control (simulation results). In particular: 1, PD without uncertainties, 2, PD with uncertainties, 3, SM without uncertainties, 4, SM with uncertainties.

Figure 14. The COMAU SMART3-S2 industrial robotic manipulator during the experimental tests.

X. CONCLUSION

In this paper, a robotic System of Systems (SoS) consisting of m distributed, cooperative and also heterogenous manipulators is considered. The idea is to make the design of the control scheme for the whole robotic system modular and composable, taking advantage from the SoS view of the system itself. To this end, a *basic module* has been defined, including a couple of robotic manipulators. Each robot can be independently controlled, with the aim of attaining a cooperative control aim. The design of the low level supervisor and of the hybrid position/force control scheme for each robot has been discussed in the paper. The new notion of safe grasp has been suitably introduced and the corresponding safe grasp condition has been defined to solve the control problem. The hybrid scheme allows one to implement decoupled position and force controllers. The proposed position and force controllers are of Sliding Mode (SM) type. The verification and the validation of our proposal have been performed by simulating the supervisor and the hybrid control scheme applied to one of the two robot manipulators, while experimentally testing the position control on a real anthropomorphic industrial robotic manipulator. The proposed controllers have been compared with conventional PD controllers.

Future research work will be devoted to design the high level supervisor, so as to coordinate a collection of basic modules, i.e. the entire robotic system viewed as a SoSoS, as mentioned in the paper. The role of the high level supervisor is that of providing the coordination and the workload sharing among the basic modules, starting from the definition of the common objectives. The proposed approach of basic modules can be valid in several fields even different from robotics, and it allows one to obtain a strategy to control and coordinate a complex large scale industrial system.

REFERENCES

[1] A. Gorod, B. Sauser, and J. Boardman, "System-of-systems engineering management: A review of modern history and a path forward," *IEEE Syst. J.*, vol. 2, no. 4, pp. 484 –499, Dec. 2008.

[2] J. Boardman and B. Sauser, "System of systems - the meaning of of," in *Proc. IEEE/SMC Int. Conf. IEEE Standard for Application and Management of the Systems Engineering ProcessSystem of Systems Engineering*, Apr. 2006.

[3] B. Siciliano and O. Khatib, Eds., *The Handbook of Robotics*. Berlin, Heidelberg, Germany: Springer, 2008, ch. 29, pp. 701–718.

[4] D. Williams and O. Khatib, "The virtual linkage: a model for internal forces in multi-grasp manipulation," in *Proc. Int. Conf. Robotics and Automation*, vol. 1, May 1993, pp. 1025–1030.

[5] K. S. Chang, R. Holmberg, and O. Khatib, "The augmented object model: cooperative manipulation and parallel mechanism dynamics," in *Proc. Int. Conf. Robotics and Automation*, vol. 1, Mar. 2000, pp. 470–475.

[6] D. Williams and O. Khatib, "Multi-grasp manipulation," in *Proc. Int. Conf. Robotics and Automation*, vol. 3, May 1995, p. 9.

[7] M. Uchiyama and P. Dauchez, "A symmetric hybrid position/force control scheme for the coordination of two robots," in *Proc. Int. Conf. Robotics and Automation*, vol. 1, Apr. 1988, pp. 350–356.

[8] E. Bassi, F. Benzi, L. Capisani, D. Cuppone, and A. Ferrara, "Characterization of the dynamical model of a force sensor for robot manipulators," in *Robot Motion and Control 2009*, ser. Lecture Notes in Control and Information Sciences, K. Kozlowski, Ed. Springer Berlin / Heidelberg, 2009, vol. 396, pp. 243–253.

[9] V. I. Utkin, *Sliding Modes in Optimization and Control Problems*. New York: Springer Verlag, 1992.

[10] C. Edwards and S. K. Spurgen, *Sliding Mode Control: Theory and Applications*. London, UK: Taylor and Francis, 1998.

[11] L. M. Capisani, A. Ferrara, and L. Magnani, "Design and experimental validation of a second-order sliding-mode motion controller for robot manipulators," *Int. J. Control*, vol. 82, no. 2, pp. 365–377, Jan. 2009.

[12] L. Fridman, "Singularly perturbed analysis of chattering in relay control systems," *IEEE Trans. Automat. Control*, vol. 47, no. 12, pp. 2079–2084, Dec. 2002.

[13] I. Boiko, L. Fridman, A. Pisano, and E. Usai, "Analysis of chattering in systems with second-order sliding modes," *IEEE Trans. Automat. Control*, vol. 52, no. 11, pp. 2085–2102, Nov. 2007.

[14] A. Levant, "Chattering analysis," *IEEE Trans. Automat. Control*, vol. 55, no. 6, pp. 1380–1389, Jun. 2010.

[15] I. Boiko, "Analysis of chattering in sliding mode control systems with continuous boundary layer approximation of discontinuous control," in *Proc. American Control Conf.*, San Francisco, CA, USA, Jul. 2011, pp. 757–762.

[16] G. Bartolini, A. Ferrara, and E. Usai, "Chattering avoidance by second-order sliding mode control," *IEEE Trans. Automat. Control*, vol. 43, no. 2, pp. 241–246, Feb. 1998.

[17] G. Bartolini, A. Ferrara, E. Usai, and V. Utkin, "On multi-input chattering-free second-order sliding mode control," *IEEE Trans. Automat. Control*, vol. 45, no. 9, pp. 1711–1717, Sep. 2000.

[18] G. Casalino, D. Angeletti, T. Bozzo, and G. Cannata, *Strategies for Control and Coordination within Multiarm Systems*. Verlag Berlin Heidelberg: Springer, 2001, pp. 1–26.

[19] O. Khatib, "Dynamic control of manipulators in operational space," in *Proc. 6th CISM-IFToMM Symposium on Theory and Practice of Robots and Manipulators*, New Delhi, India, Dec. 1983, pp. 1128–1131.

[20] B. Siciliano, L. Sciavicco, L. Villani, and G. Oriolo, *Robotics-Modelling, Planning and Control*, 3rd ed. London, UK: Springer-Verlag, 2009.

[21] A. Calanca, L. Capisani, A. Ferrara, and L. Magnani, "Mimo closed loop identification of an industrial robot," *IEEE Trans. Control Syst. Technol.*, vol. 19, no. 5, pp. 1214–1224, Sep. 2011.

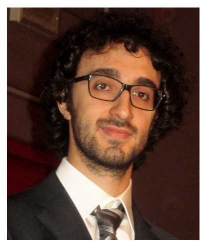

Gian Paolo Incremona received the Master Degree (with honor) in Electrical Engineering from the University of Pavia, Italy in 2012. He was a student of the *Almo Collegio Borromeo* of Pavia, and of the class of *Science and Technology* of the Institute for Advanced Studies *IUSS* of Pavia. He is now a Ph.D. Candidate in Electronics, Electrical and Computer Engineering at the Identification and Control of Dynamic System Laboratory of the University of Pavia. His research deals with industrial robotics, real-time physical systems, optimal control and variable structure control methods of sliding mode type.

Gianluca De Felici has a position as Senior Laboratory Technician at the Identification and Control of Dynamic System Laboratory of the University of Pavia. After graduating in Electronics, he actively participated in research activities in industrial automation, packaging and automatic handling systems.

Antonella Ferrara is Full Professor of Automatic Control at the University of Pavia. Her research deals with sliding mode and nonlinear control with application to traffic, automotive and robotics. She has authored/co-authored more than 260 papers, including 83 journal papers. She was *Associate Editor* of the *IEEE Transactions on Control Systems Technology* and of the *IEEE Transactions on Automatic Control*. She is *Senior Member* of the *IEEE Control Systems Society*, member of the *IEEE Technical Committee on Variable Structure and Sliding Mode Control* and of the *IEEE Robotics and Automation's Technical Committee on Autonomous Ground Vehicles and Intelligent Transportation Systems*.

Ezio Bassi was born in Voghera, Italy, in 1951 and received the Dr. Ing. Degree in Ingegneria Elettrotecnica from the University of Pavia in 1976, where he serves since 2003 as a Full Professor of Electrical Machines and Drives. His research interests include the modelling of converter-fed electrical machines, the identification and regulation procedures of adjustable speed drives with numeric algorithms, specially for applications with robotic actuators and linear drives, the integration of drives with other system components through field busses and communication protocols even for diagnostic purposes. Prof. Bassi is a member of *CEI Technical Committee 301- Electrical Drives*.